ORIGINAL RESEARCH

Population pharmacokinetics of pegaptanib sodium (Macugen®) in patients with diabetic macular edema

Anthony S Basile[1]
Matthew M Hutmacher[2]
Kenneth G Kowalski[2]
Kuan Y Gandelman[3]
Dana J Nickens[1]

[1]Clinical Pharmacology, Specialty Care Business Unit, Pfizer Inc, San Diego, CA, USA; [2]Ann Arbor Pharmacometrics Group, Ann Arbor, MI, USA; [3]Clinical Pharmacology, World Wide Biopharmaceuticals, Pfizer Inc, New York, NY, USA

Objective: Population pharmacokinetic modeling of pegaptanib was undertaken to determine influence of renal function on apparent clearance.

Methods: In a randomized, double-masked multicenter trial, intravitreal pegaptanib (0.3, 1.0, or 3.0 mg/eye) was administered in patients with diabetic macular edema every 6 weeks for 12–30 weeks. A one-compartment model with first-order absorption, distribution volume, and clearance was used to characterize the pegaptanib plasma concentration–time profile.

Results: In 58 patients, increases in area under the concentration–time curve (AUC) to end of the dosing interval (AUC_{0-tau}) and maximum concentration with repeat doses were <6%, indicating minimal plasma accumulation. Sex and race did not have clinically significant effects on pegaptanib exposure. In the final model, the AUC extrapolated to infinite time and maximum concentration increased by ≥50% in older patients (aged >68 years) relative to younger patients due to decreases in creatinine clearance (CRCL), a significant predictor of clearance. Pegaptanib clearance was reduced by 29% when CRCL decreased by 50%. The change in exposure with CRCL (range, 0–190 mL/minute) was < 10-fold with 0.3–3.0 mg doses.

Conclusion: While pegaptanib clearance and AUC were significantly influenced by CRCL, the predicted exposure in patients with renal insufficiency or renal failure shows no evidence that a dose adjustment is warranted, given the tenfold margin of safety observed over the dose range of 0.3–3.0 mg.

Keywords: clearance, diabetic macular edema, pegaptanib, population pharmacokinetics, renal function

Introduction

Diabetic macular edema (DME) is an edematous thickening of the macular region of the retina that is associated with reduction in visual acuity. DME frequently accompanies diabetic retinopathy, which is a retinal angiopathy associated with type 1 and type 2 diabetes mellitus. Diabetic retinopathy is a leading cause of blindness in Western societies,[1] and is expected to increase as the anticipated prevalence of diabetes rises to 4.4% in 2030.[2]

There is substantial evidence implicating vascular endothelial growth factor (VEGF) as a significant contributor to the increase in vascular permeability and angiopathy observed in diabetic retinopathy and DME. One of the biological activities of VEGF is to increase vascular permeability by specifically binding to receptors on vascular endothelial cells.[3] Intravitreal (IVT) injections of $VEGF_{165}$, the primary VEGF isoform involved in ocular angiopathies,[4,5] causes blood–retinal barrier breakdown and microaneurysm formation.[6] Further, retinal levels of $VEGF_{165}$ rise within 1 week of the onset

Correspondence: Dana Nickens
Clinical Pharmacology, Specialty Care Business Unit, Pfizer Inc, 10777 Science Center Drive, San Diego, CA 92121, USA
Tel +1 858 526 4840
Fax +1 858 678 8263
Email dana.j.nickens@pfizer.com

of DME and are temporally correlated with the blood–retinal barrier breakdown observed in animal models of diabetic retinopathy.[7] Blocking the actions of VEGF in these models reduced the retinal vascular permeability and blood–retinal barrier breakdown to levels observed in healthy, nondiabetic animals. Finally, VEGF levels are reportedly elevated in the retina[8] and aqueous humor[9] of patients with macular edema, with a significant correlation between VEGF concentrations and disease severity.

Together, these data support the use of anti-VEGF$_{165}$ therapy for the treatment of patients with DME. One such agent is pegaptanib sodium (Macugen®; Eyetech Inc, Palm Beach Gardens, FL, USA), which is currently approved for the treatment of neovascular, age-related macular degeneration (AMD),[10] in which VEGF is known to play an important role. Pegaptanib is a pegylated oligoribonucleotide (aptamer) that binds with high specificity and affinity to VEGF$_{165}$, sequestering, and therefore preventing VEGF$_{165}$ from activating its receptor.[10] It is hypothesized that the action of pegaptanib as a functional antagonist of VEGF$_{165}$ could play a significant role in treating DME by suppressing VEGF-induced vascular leakage and retinal edema.

Oligonucleotides are cleared from the body primarily by renal elimination,[11,12] with hepatic clearance (CL) acting as a secondary pathway.[13,14] Pegaptanib is believed to be eliminated through similar processes. The renal elimination pathway for oligonucleotides may be impaired in diabetic patients, who suffer from a high incidence of renal insufficiency and end-stage renal failure.[15] Moreover, renal function declines steadily with age, independent of other disease processes.[16] Thus, the impairment of renal function in patients with DME may increase systemic exposure to pegaptanib following IVT administration, requiring an adjustment in dose. Therefore, a population pharmacokinetic (PK) analysis based on plasma samples was performed using data obtained from diabetic patients treated for DME, in order to assess the impact of renal function on CL and systemic exposure (area under the concentration–time curve [AUC] and maximum concentration [C$_{max}$]) to pegaptanib.

Methods
Ethics
The investigation contributing to this population PK analysis was conducted in accordance with the rules, regulations, and ethical practices laid out in the Helsinki Declarations and local legal and regulatory bodies pertinent to the conduct of trials in new therapeutics. All study protocols were reviewed and approved by the Institutional Review Boards of the study centers involved. Moreover, all patients or their legal representative provided written informed consent prior to their enrollment in these studies.

Study design
EOP1005 was a randomized, double-masked, sham injection-controlled, dose-finding, multicenter trial conducted using a parallel-group design. Patients were randomized to receive one of three doses of pegaptanib (0.3 mg, 1.0 mg, or 3.0 mg) or sham control injections (n=44, 44, 42, and 42, respectively). The sham-control group had an empty syringe with no needle applied to the eye, which was pressed to simulate an injection. Patients received a minimum of three IVT pegaptanib injections or sham-control applications at weeks 0, 6, and 12. Additional injections were permitted at weeks 18, 24, and 30 at the discretion of the investigator, for a possible maximum of six IVT pegaptanib or sham administrations.

In study EOP1005, the pegaptanib arms were compared with the sham arm to evaluate efficacy. The primary efficacy endpoint was the change in retinal thickness between baseline and week 36 as measured in the central subfield by optical coherence tomography. The key secondary efficacy endpoint was the change in best-corrected visual acuity between baseline and study week 36. The resulting clinical efficacy of pegaptanib in the treatment of DME has been previously published.[17.]

PK sampling and drug concentration assays
Serial blood samples for the determination of pegaptanib concentrations were collected after the first and third pegaptanib or sham injections at predose, 4 hours, 24 hours, and 1, 3, and 6 weeks postdose (detailed nominal schedule are presented in Table S1). All plasma samples were kept frozen (at −20°C) after preparation and until shipment. A good laboratory-practice-validated, dual hybridization assay was used to determine plasma pegaptanib concentrations (PPD Development, Richmond, VA, USA). The assay maintained a lower limit of quantification (LLOQ) of 0.5 ng/mL.

PK modeling
The parameters of the non-linear, mixed-effect models were estimated using NONMEM® version VII (ICON Development Solutions, Dublin, Ireland).[18] SAS 9.1.3 (Service Pack 4 XP_PRO platform; SAS Institute, Cary, NC, USA) and S-Plus 7.0 (TIBCO Software Inc, Palo Alto, CA, USA) were used to process the data and to perform simulations.[19]

Graphical analysis of the data or model output was performed using S-Plus. Concentration data below LLOQ (BLQ) were incorporated by formally specifying the likelihood and treating these data as censored observations (M3 method in NONMEM).[20,21]

A one-compartment model with first-order absorption was used to describe the pegaptanib plasma concentration–time profiles. A two-compartment model did not improve prediction, and only minimal information on a second compartment was available from the dataset. The structural base model was parameterized using the apparent steady-state volume (V), CL, and acceleration constant (Ka), which described the transfer of pegaptanib from the ocular compartment to systemic circulation.

Flip-flop kinetics were assumed in the model, based on preclinical studies indicating that the terminal half-life ($T_{1/2}z$) of pegaptanib is shorter following intravenous rather than IVT administration.[22] To maintain flip-flop kinetics, population parameters were not constrained. Preclinical studies estimated the bioavailability of pegaptanib after IVT administration to be 70%–100%. The ratio of Ka and the elimination rate constant

$$K_e = CL/V \qquad (1)$$

estimates were greater than an order of magnitude, indicating that appropriate starting values would converge to proper estimates. Diagnostic plots were qualitatively inspected to evaluate the quality of the fit. Random effect models were constructed, with the random effect for interindividual variability applied to CL, V, and Ka, and random effects for inter-occasion variability applied to Ka.

A full model was constructed by adding a targeted set of covariates (Equations 2–4) to the base model because of the relatively small number of subjects (N=58) enrolled. Clinical judgment was used to determine which covariates were tested for their influence on specific PK parameters.

The parameter equations for the full model were:

$$CL_i = exp(\theta_1)\left(\frac{CRCL_i}{80}\right)^{\theta_5}\left(\frac{WT_i}{85}\right)^{\theta_6}$$
$$exp(\theta_7 \times SEX_i)\left(\frac{AGE_i}{65}\right)^{\theta_8} exp(\eta_i^{(CL)}) \qquad (2)$$

$$V_i = exp(\theta_2)\left(\frac{WGT_i}{85}\right)^{\theta_9} exp(\theta_{10} \times SEX_i) exp(\eta_i^{(V)}) \qquad (3)$$

$$Ka_i = exp(\theta_3)\left(\frac{AGE_i}{65}\right)^{\theta_{11}} exp(\theta_{12} \times SEX_i) exp(\eta_i^{K_a}) \qquad (4)$$

All the covariate effects were added and estimated simultaneously to establish a full PK model, which was subjected to Wald's approximation method (WAM).[23]

The WAM procedure identified a subset of parsimonious PK models constructed using combinations of the eight covariates in the full model. WAM was used to approximate Schwarz's Bayesian criterion (SBC) and to rank all the models relative to the maximum SBC. The top 15 ranked models were fitted using NONMEM to calculate the likelihood function-based SBC estimates, with the final parsimonious model selected on the basis of the maximum NONMEM-based SBC.

The distributions of the percentages of BLQ concentrations were compared with those observed in the actual data. Geometric means of the simulated data greater than LLOQ (0.5 ng/mL) were computed for each replicate trial by time windows. The distributions of these conditional geometric means were compared with the geometric means of non-BLQ data, which were computed using the same time window. A predictive check was also performed to evaluate the quality of the model fit. Data were simulated using the final model in NONMEM for 500 replicate trials that were similar in design to the EOP1005 trial in terms of dosing, sampling times, and covariates. The distributions of the percentages of BLQ concentrations were compared with those observed in the actual data. The comparisons were reported for ad hoc time windows because of the sparse sampling times. Geometric means of the simulated data greater than the LLOQ were also computed for each replicate trial by time windows. The distributions of these conditional geometric means were compared with the geometric means of non-BLQ data, which were computed using the same time window.

The final model was used to predict estimates of standard noncompartmental analysis (NCA)–type parameters. The empirical Bayes' predictions of the random effects, $\eta^{(\cdot,p)}$, were used to generate individual predictions of the compartmental PK parameters. These predictions were entered into the following equations to generate NCA parameter predictions for a single injection of 0.3 mg pegaptanib (Equations 5–7),

$$AUC_{(0-inf)i}^{(p)} = \frac{1,000 \times 0.3\,mg}{CL_i^{(p)}}$$
$$T_{max_i^{(p)}} = \frac{\ln(Ke_i^{(p)}) - \ln Ka_i^{(p)}}{Ke_i^{(p)} - Ka_i^{(p)}} \qquad (5)$$

$$C_{max_i^{(p)}} = \frac{1,000 \times 0.3\,mg \times Ka_i^{(p)}}{\left(Ke_i^{(p)} - Ka_i^{(p)}\right)} \times \left[exp\left(-Ka_i^{(p)} \times T_{max^{(p)}}\right) \right.$$
$$\left. - exp\left(-Ke_i^{(p)} \times T_{max^{(p)}}\right) \right] \tag{6}$$

$$T_{\frac{1}{2}}z_i^{(p)} = \frac{24 \times ln(2)}{Ka_i^{(p)}} \tag{7}$$

where AUC_{0-inf} is AUC from time 0 to infinity, T_{max} is the time at which the maximum concentration was predicted for a single dose, C_{max} is the maximum concentration predicted for a single dose, and $T_{1/2}z$ reflects the terminal elimination half-life. These NCA parameter predictions were log-transformed to calculate geometric mean and percent coefficient of variation by covariate groups.

Finally, pegaptanib CL at clearance (CRCL) <30 mL/minute was predicted using a simplified power model:

$$CL_i = exp\theta_1 \left(\frac{CRCL_i}{80}\right)^{\theta_5} exp\left(\eta_i^{(CL)}\right) \tag{8}$$

which predicts CL_i to be 0 when $CRCL_i = 0$; and a linear model:

$$CL_i = \left[exp\left(\theta_1\right) + SLP \times \left(CRCL_i - 80\right) \right] exp\left(\eta_i^{(CL)}\right) \tag{9}$$

For both models, $exp(\theta_1)$ represents the typical individual prediction of CL at $CRCL_i = 80$ mL/minute (mean of all dose groups rounded to nearest 10). The slope parameter (SLP) for CRCL was parameterized as:

$$SLP = \frac{1}{80} exp(\theta_1) exp(-exp(\theta_5)) \tag{10}$$

which allows θ_5 (relating the changes in CRCL to changes in CL) to range from $-\infty$ to ∞ while constraining $SLP > 0$. As a result, $CL_i > 0$. Maintaining a feasible prediction of CL_i over this range is important, because a smoothed parametric bootstrap procedure was used to generate confidence intervals (CIs). For this procedure, the sampling distribution of the parameter estimates was assumed to be multivariate normal with a covariance matrix equal to the covariance matrix of the estimates, which in turn is derived from the Hessian matrix (R matrix in NONMEM). Parameters were sampled from this distribution and plugged into the model to yield typical individual predictions per replicate sampled. The 5th and 95th percentiles of the distributions were computed and plotted as the 90% CI. The restriction of $SLP > 0$ is supported

by the selection of CRCL as a predictive covariate for CL during covariate model development. This selection indicates a "significant" relationship between CL and CRCL.

Results

A total of 550 observations of pegaptanib plasma concentrations from 58 patients supported the development of the population PK models. The number of patients and a summary of covariates are displayed by dose group in Table 1. Because ~26% of the data were BLQ (Table S2), a component for censoring was added to the likelihood function in order to appropriately incorporate these data into the model. The 0.3 mg pegaptanib treatment group had the largest number of BLQ observations (47%) compared with the other arms (<19%). Race effects are included in Table 1 for completeness, but were not considered in the covariate analysis

Table 1 Summary of covariate data

	Pegaptanib dosage			Total
	0.3 mg n=20	1.0 mg n=23	3.0 mg n=15	N=58
Discrete, n (%)				
Race				
Asian	1 (1.72)	1 (1.72)	0 (0.00)	2 (3.45)
Black	3 (5.17)	3 (5.17)	2 (3.45)	8 (13.79)
Hispanic	1 (1.72)	1 (1.72)	2 (3.45)	4 (6.90)
White	15 (25.86)	18 (31.03)	11 (18.97)	44 (75.86)
Total	20 (34.48)	23 (39.66)	15 (25.86)	58 (100.00)
Sex				
Female	11 (18.97)	16 (27.59)	5 (8.62)	32 (55.17)
Male	9 (15.52)	7 (12.07)	10 (17.24)	26 (44.83)
Total	20 (34.48)	23 (39.66)	15 (25.86)	58 (100.00)
Continuous				
Age, years				
Mean	60.75	62.83	61.27	61.71
Median	60.50	64.00	62.00	61.50
SD	11.80	12.74	10.05	11.61
Minimum	44.00	27.00	42.00	27.00
Maximum	89.00	81.00	76.00	89.00
CRCL, mL/min				
Mean	85.12	66.38	85.09	77.68
Median	77.10	64.31	73.27	70.48
SD	39.77	25.78	29.03	32.80
Minimum	36.07	29.94	46.18	29.94
Maximum	189.54	123.49	135.96	189.54
Weight, kg				
Mean	83.46	85.33	92.63	86.58
Median	84.45	83.50	90.30	85.15
SD	19.77	14.24	24.46	19.21
Minimum	47.20	59.50	51.10	47.20
Maximum	123.50	109.40	129.40	129.40

Notes: All covariates summary measures are from baseline/screening (prior to treatment) values.
Abbreviations: N, total number of patients; n, number of patients in subgroup; SD, standard deviation; CRCL, creatinine clearance based on the Crockroft-Gault formula; min, minute.

because the majority of patients were white (n=44 of 58). The 1.0 mg treatment group appeared to have lower CRCL values than the other treatment groups, but the body-weight distribution for this group was comparable to the other groups. The age distribution and number of males to females also appeared to be similar across treatment groups.

A one-compartment model with first-order absorption adequately characterized the pegaptanib concentration–time profile following IVT administration, and was used as the base model. The WAM[22] algorithm was applied to the full model, and resulted in a model with a CRCL effect on CL and sex effect on Ka. This model was selected as the final model because it maximized the Wald-based[23] (−32.379 vs −33.012 for next-best model) and NONMEM-based[17] (−31.300 vs −31.746 for next-best model) SBCs. The observed concentrations and model predictions as determined using the final model for the first and third doses of pegaptanib 0.3 mg, 1.0 mg, and 3.0 mg per eye administered every 6 weeks are presented in Figure S1. The increase in AUC from time 0 to end of the dosing interval (AUC_{0-tau}) and C_{max} from the first to third dose was <6%, consistent with minimal accumulation of pegaptanib with repeat dosing. Predictions of these parameters at steady state, based on a fixed inter-dosing interval of 6 weeks, also suggested minimal pegaptanib accumulation.

The NCA parameters were calculated using the final model; the results for a normalized prediction to the 0.3 mg dose of pegaptanib are displayed in Table 2. Using these normalized predictions, it was found that the sex had small (<20%) numerical effects on AUC_{0-inf}, C_{max}, or $T_{1/2}$ z. Although males had a higher C_{max} than females, they displayed lower plasma concentrations during the terminal phase (Figure 1). In contrast, the covariates age, weight, and CRCL showed larger numerical changes in AUC. Given the observed age distribution, older patients (aged >68 years) had a 63% higher AUC relative to younger patients (aged ≤57 years). For the observed weight range in this study, patients with lower weight (≤79 kg) had a 49% higher AUC than those with higher weight (>93 kg). Given the observed CRCL distribution for the study, patients with a CRCL of ≤63 mL/minute had a 61% higher AUC than patients with a CRCL of >86 mL/minute. Age had the greatest influence on C_{max}, causing a 50% increase in patients aged >68 years relative to those aged ≤57 years. This increase in C_{max} most likely reflects the age-related decline in CRCL superimposed upon any diabetic nephropathy.[15,16]

All CRCL values in patients participating in this study varied from 30 to 190 mL/minute (median 70.5 mL/minute). The temporal changes in pegaptanib exposure for patients

Table 2 Non-compartmental analysis parameter predictions for the final model scaled to 0.3 mg pegaptanib

	n	AUC_{0-inf}, ng·h/mL			C_{max} (single dose), ng/mL			T_{max} (single dose), h			$T_{1/2}$z, d		
		Mean	Med	%CV	Mean	Med	%CV	Mean	Med	%CV	Mean	Med	%CV
Sex													
Female	322	1,586	1,757	50.0	4.3	4.7	44.6	91.5	103.0	47.3	7.1	7.2	10.2
Male	26	1,635	1,561	23.4	5.0	5.2	24.6	81.4	92.4	31.2	6.5	6.4	14.3
Race													
White	44	1,567	1,686	43.8	4.5	4.7	38.7	85.3	92.7	41.5	6.9	6.9	13.0
Black	8	1,843	1,961	27.1	5.6	6.1	28.9	85.9	94.3	37.2	6.4	6.1	12.0
Hispanic	4	1,609	1,707	25.3	3.8	3.5	39.7	123.0	115.4	40.8	7.5	7.6	10.8
Asian	2	1,635	1,635	5.0	5.3	5.3	2.2	65.9	65.9	24.4	6.6	6.6	14.1
Age, y													
≤57	21	1,279	1,509	52.1	3.6	3.8	47.9	84.4	92.7	45.4	6.9	6.6	12.0
57–68	21	1,708	1,710	22.3	5.1	4.9	22.9	82.7	83.4	39.4	6.6	6.6	12.3
>68	16	2,004	1,969	22.5	5.4	5.3	19.9	96.1	99.0	37.5	7.1	7.3	14.5
Weight, kg													
≤79	20	1,960	2,010	23.2	5.5	5.4	23.2	93.0	94.7	33.9	6.8	6.6	12.4
79–93	19	1,553	1,657	40.1	4.6	5.1	39.0	78.2	80.7	50.5	6.8	7.2	14.8
>93	19	1,351	1,418	46.1	3.8	3.9	40.3	89.6	95.3	37.1	6.9	6.7	12.1
CRCL (mL/min)													
≤63	20	1,951	1,989	25.9	5.5	5.9	26.1	91.8	97.5	31.4	6.8	6.6	13.0
63–86	19	1,605	1,744	40.8	4.5	4.8	37.2	87.4	93.7	55.1	6.9	7.2	14.9
>86	19	1,314	1,509	43.0	3.9	4.3	40.4	81.3	91.7	34.1	6.8	6.7	11.4
Total	58	1,608	1,727	40.0	4.6	4.8	37.5	86.8	92.7	41.0	6.8	6.7	12.9
Sim total[a]		1,592	1,590	45.2	4.5	4.5	40.8	85.0	86.7	51.1	6.8	6.8	19.7

Note: [a]Simulation considered 100,000 virtual subjects.
Abbreviations: n, number of patients in subgroup; AUC_{0-inf}, area under the concentration–time curve from time 0 to infinity; h, hour; C_{max}, maximum concentration; T_{max}, time at maximum concentration; $T_{1/2}$z, terminal half-life; d, days; Med, median; CV, coefficient of variation; y, years; CRCL, creatinine clearance; min, minute; Sim, simulation.
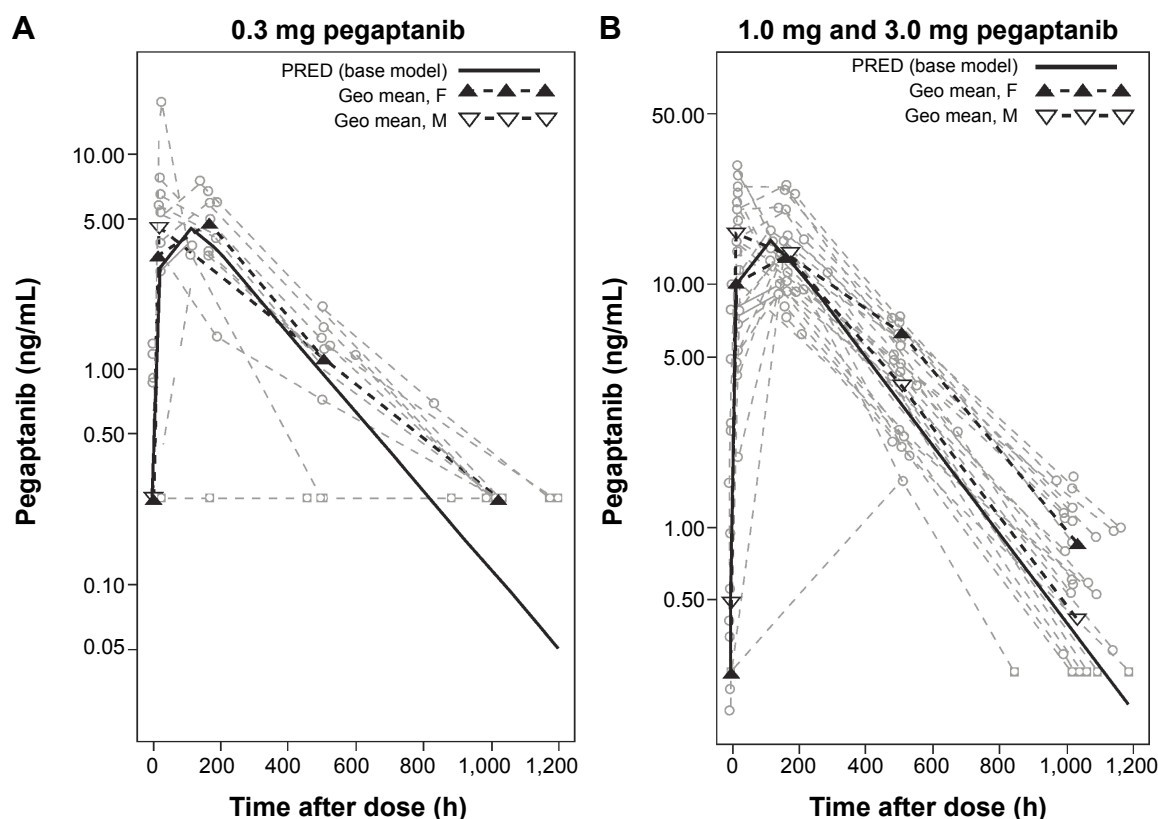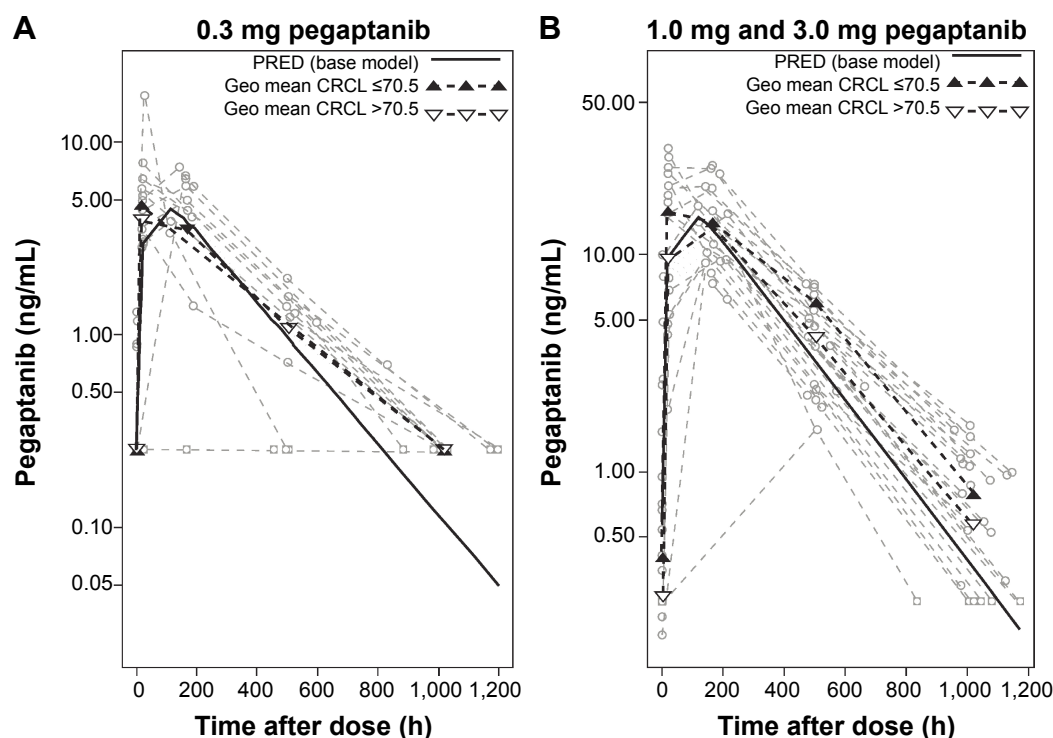
Figure 1 Influence of sex on plasma pegaptanib levels over time.

Notes: (**A**) Patients treated with a single dose of 0.3 mg pegaptanib/eye had a rate of 47% below the lower limit of quantification (BLQ), and therefore, these data were not pooled by dose-normalization. (**B**) Patients in the 1.0 mg and 3.0 mg pegaptanib/eye cohorts had similar rates of BLQ readings (17% and 8%, respectively), and were pooled by dose-normalizing, allowing for greater statistical power. This provided evidence that males treated with either 1.0 mg or 3.0 mg pegaptanib had a higher maximum concentration (C_{max}), but lower plasma concentrations during the terminal phase and thus, a faster terminal elimination rate than females.

Abbreviations: F, females; h, hour; Geo, geometric; M, males; PRED, prediction.

stratified into CRCL groups above and below the median value indicated that plasma pegaptanib concentrations showed a trend toward higher concentrations in patients with lower CRCL values (Figure 2) in the groups receiving pegaptanib 1.0 mg and 3.0 mg doses per eye. The predicted CL values ranged from 0.124 to 0.305 over the observed range of CRCL values (Table 1). The changes in CL are less than proportional to changes in CRCL, as indicated by the ratio of 2.46 for CL compared with 6 for CRCL over the range of both variables. These results also apply for the predicted AUC_{0-inf}, whose values ranged from 2,419 to 983 ng·hour/mL over the same series of CRcl values (Figure S2). The AUC for patients with CRCL of 30–40 mL/minute was predicted to be less than twofold higher than in patients with CRCL of 80 mL/minute. The relationship between the pegaptanib CL/AUC and the CRCL predicted by the final model for a typical individual (random effect set to 0) is shown in Figure 3. The ratio of CL/AUC for CRCL of 30–190 mL/minute to the CL/AUC predicted for a patient with a CRCL of 80 mL/minute ranges from 0.62 to 1.53.

The AUC in patients with a low CRCL was predicted to be less than twofold higher than in patients with a CRCL of 80 mL/minute. Although no patients were available with a CRCL <30 mL/minute, predictions of the systemic exposure to pegaptanib were simulated (Figure 4). The empirical Bayes' predictions were nearly indistinguishable for the two models, as were the typical individual predictions over the range of observed CRCL (30–190 mL/minute). The 90% CI for the power model was larger, and generally contains the prediction and 90% CI for the linear model. The two models started to diverge at CRCL <30 mL/minute (Figure 4), but the difference in the CL prediction was only 0.0349 L/hour at a CRCL of 10 mL/minute (CL 0.107 L/hour for the linear model and 0.0722 L/hour for the power model). The predicted ratio of AUC at a CRCL of 10 mL/minute by model was 1.484, which indicates that the power model predicts a 48% higher AUC relative to the linear model (for a CRCL of 10 mL/minute). Since the study did not include data on patients with CRCL<30, predictions in this range should viewed with caution and in light of the variability associated

Figure 2 Influence of the covariate creatinine clearance (CRCL) on plasma pegaptanib levels over time.
**Notes:** Data from patients were stratified based on CRCL values >70.5 mL/min or ≤70.5 mL/min, which was the median CRCL value for this study. (**A**) Patients treated with a single dose of 0.3 mg pegaptanib/eye had a rate of 47% below the lower limit of quantification (BLQ), and therefore, these data were not pooled by dose normalization. (**B**) Patients in the 1.0 mg and 3.0 mg pegaptanib/eye cohorts had similar rates of BLQ readings (17% and 8%, respectively), and were pooled by dose normalizing, allowing for greater statistical power. This provided evidence that patients with a CRCL ≤70.5 mL/min had higher maximum concentration values and higher plasma concentrations than those with CRCL >70.5 mL/min.
Abbreviations: h, hour; Geo, geometric; min, minute; PRED, prediction.
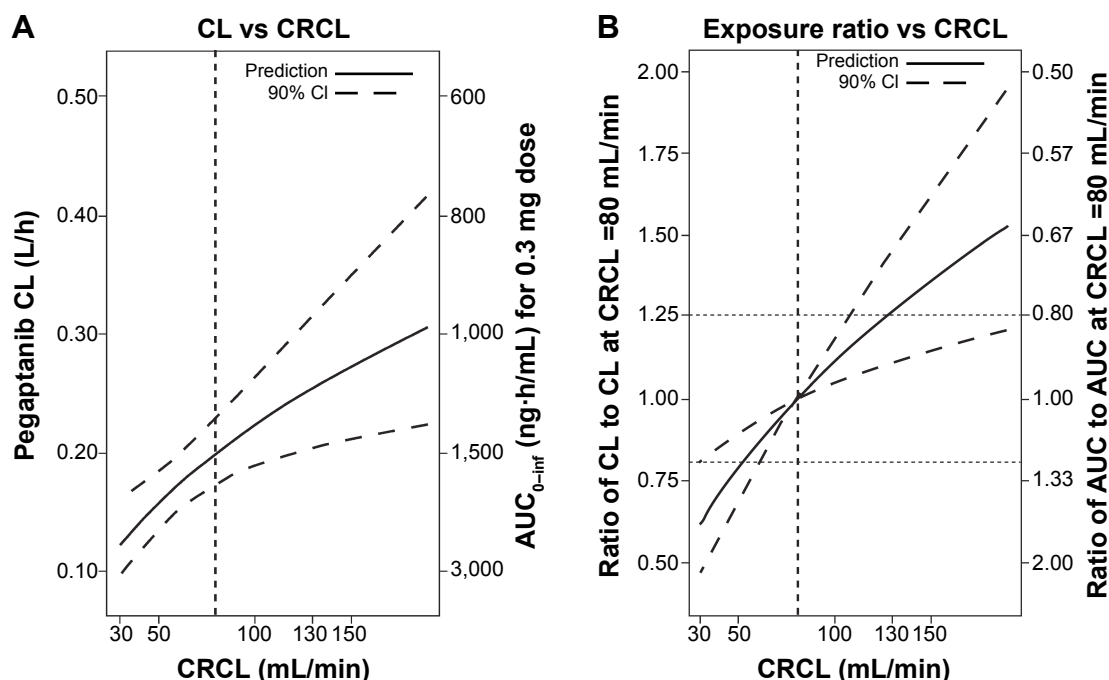
Figure 3 (**A**) Influence of creatinine clearance (CRCL) on the predicted pegaptanib exposure for a typical individual. The predictions are based on the final model, with η set to 0 for a typical individual. (**B**) The ratio of clearance (CL) for a 0.3 mg dose to the CL predicted for a patient with a CRCL of 80 mL/min. The ratio of area under the concentration–time curve (AUC) for a 0.3 mg dose to the AUC predicted for a patient with a CRCL of 80 mL/min is also shown. The 90% confidence intervals (CIs) are displayed as dashed lines in both panels. These were computed by sampling parameter estimates from a multivariate normal distribution (n=10,000) with a covariance matrix equal to the covariance matrix of the estimates from the full working model to avoid overly narrow CI ranges.
Abbreviations: AUC_{0-inf}, area under the concentration–time curve from time 0 to infinity; h, hour; min, minute; vs, versus.
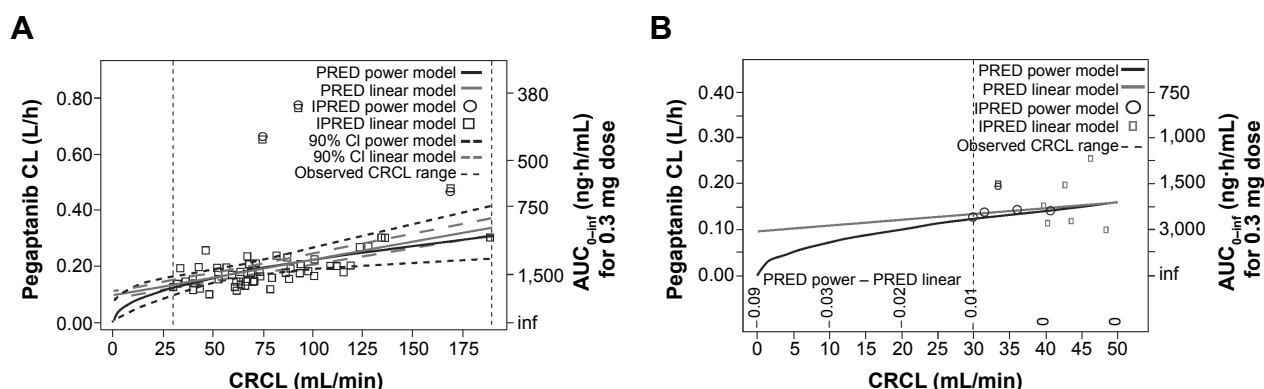
Figure 4 Clearance (CL) and area under the concentration–time curve (AUC) at creatinine clearance (CRCL) <30 mL/min predicted using two models.
Notes: (**A**) In order to gain insights into the systemic exposure to pegaptanib in patients with severe renal insufficiency or renal failure, two models (a linear model and a simplified non-linear power model) were used to predict CL and AUC at CRCL <30 mL/min. Note that the 90% CIs for both models overlap over virtually the entire range of CRCL. (**B**) Closer examination of the CL and AUC at CRCL <30 mL/min. The non-linear power model predicts a rapid decline in pegaptanib CL and divergence from the linear model prediction at CRCL <15 mL/min. In contrast, the linear model predicts residual pegaptanib clearance would occur at CRCL <15 mL/min, consistent with the presence of secondary, non-renal elimination pathways for pegaptanib.
Abbreviations: AUC_{0-inf}, area under the concentration–time curve from time 0 to infinity; CI, confidence interval; h, hour; inf, infinity; IPRED, individual prediction; min, minute; PRED, prediction.

with those predictions. Also, this analysis does not directly provide information about any type of non-renal CL.

Although CRCL had a significant effect on C_{max} (Table 2), this effect was similar in both sexes (Figure S3). The C_{max} ranged from 2.9 to 5.9 ng/mL in females and 3.5 to 6.9 ng/mL in males. The range of C_{max} values varied less than twofold over the range of CRCL observed, suggesting that sex-based differences in C_{max}, while they may be numerically different, are probably not clinically meaningful. A summary of the influence of all the investigated intrinsic covariates is provided in Figure 5. In most cases, the effect of the intrinsic covariate on either AUC or C_{max} is not significantly different from the reference values, as indicated by the overlap of the 90% CI with the dotted vertical line at 1.0 in Figure 5.

Discussion

Although other mechanisms, including hepatic and splenic uptake, play secondary roles in elimination, oligonucleotides, such as pegaptanib, a $VEGF_{165}$-sequestering aptamer, are eliminated primarily by renal CL. Pegaptanib was previously approved for the treatment of neovascular AMD[10] and is being investigated for the treatment of DME. Unlike the AMD population, which presents with age-dependent decrements in renal function, the DME population can manifest renal insufficiency due both to age and diabetic nephropathy. The impact of renal function and other covariates (eg, sex) on the systemic exposure to pegaptanib in diabetic patients may require an adjustment in pegaptanib dosing. Therefore, a population PK study was performed using data from a clinical investigation of pegaptanib PK in patients with diabetic retinopathy and DME to determine the influence of

CRCL, as an index of renal function, and other covariates on pegaptanib CL following IVT administration.

As previously observed in the population PK study in AMD patients,[24] a single-compartmental model incorporating CL, V, and Ka adequately characterized the pegaptanib concentration–time profile following IVT administration in diabetic patients. The limited number of patients (N=58) enrolled in the current study and the relatively large percentage of samples that were BLQ (particularly in the cohort receiving the 0.3 mg dose) required the use of a censored likelihood component to incorporate all of the data into the model, which was then normalized to the 0.3 mg dose of pegaptanib. Although sex was included in the final model as a statistically significant effect on absorption, the model-predicted NCA parameters showed that influence of sex on systemic pegaptanib exposure was small (decreases of 21% in C_{max} and 5% in AUC among males and females) and not likely to be clinically significant (for C_{max} or AUC). However, age and body weight, which significantly influence CRCL, impacted systemic exposure to pegaptanib. The covariate search process indicated that these influences were primarily due to change in CRCL, which is associated with renal function.

CRCL significantly influenced AUC_{0-inf} and C_{max}, with an approximately twofold change in these parameters over the observed range of CRCL. However, the change in CL that this represents is expected to result in substantially less than the tenfold increase in systemic exposure (AUC) observed after administration of the well-tolerated 3.0-mg dose of pegaptanib. This was true not only when based on the data obtained from direct observation in patients with
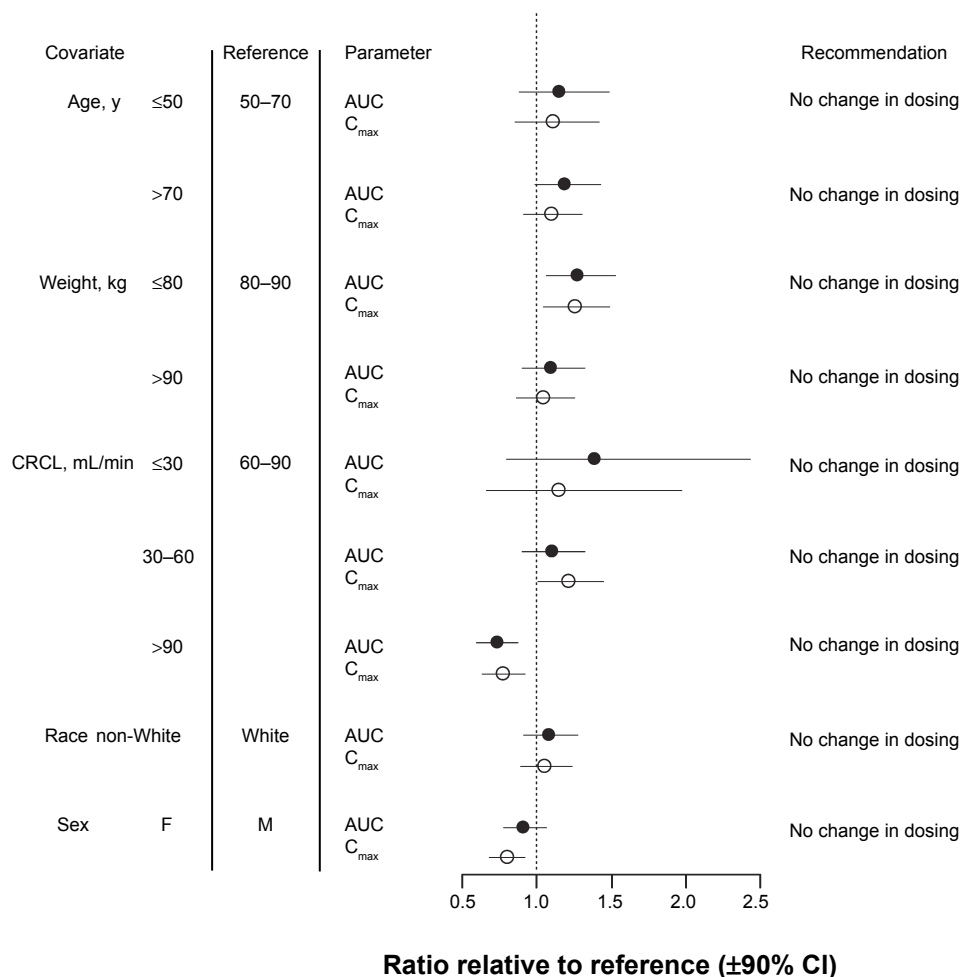
Figure 5 Forest plot summarizing the influence of diabetic macular edema on the systemic exposure to pegaptanib.
Notes: The mean ± 90% CI of ratios of the area under the concentration–time curve (AUC; black circle) and maximum concentration (C_{max}; white circle) for the various covariates relative to the reference values for these pharmacokinetic parameters are shown. As an example, if the AUC for a patient with a body weight ≤60 kg was the same as that for the reference population of 60–70 kg, the value indicated on the chart would be 1.
Abbreviations: CI, confidence interval; CRCL, creatinine clearance; F, female; M, male; min, minute; y, years.

moderate renal insufficiency (CRCL 30 mL/minute), but was also predicted for individuals suffering from renal failure (CRCL <15 mL/minute). Within the context of the safety profile of pegaptanib in patients with DME, we conservatively estimated that adjustments to pegaptanib dosing should not be required, even in patients with severe renal insufficiency or renal failure.

The PK of pegaptanib in patients with DME is qualitatively similar to that observed in those with AMD,[24] where the ratio of CL for the lowest and highest CRCL values was 2.3-fold. In that population, age as opposed to sex was a predictor of Ka. Nonetheless, these covariates and those affecting CL were not considered to be clinically meaningful relative to the safety margin established for the 0.3 mg/eye regimen in the current study. In most cases, the effect of the intrinsic covariate on either AUC or C_{max} is not significantly different from the reference values and, in all cases, the change in systemic

exposure is less than that observed following administration of the well-tolerated 3.0 mg dose of pegaptanib (reference ratio =10, data not shown). It is concluded that the results of this population PK analysis of pegaptanib in patients with DME are similar to those observed in AMD patients in that they do not warrant an adjustment of the pegaptanib dose in patients with renal insufficiency, nor do they indicate an alternative to dosing every 6 weeks.

In the current study, an analysis of pegaptanib PK in a population of patients with DME was performed using a single-compartment model. Predicted parameters from this model indicated that pegaptanib did not accumulate in the plasma after multiple doses, and that the covariates race and sex had no clinically significant impact on the PK of pegaptanib. While pegaptanib CL and AUC were significantly influenced by CRCL, the increase in these parameters was such that it can be concluded that no dose adjustment

is warranted for patients with severe renal insufficiency or renal failure, given the tenfold margin of safety observed over the dose range of 0.3–3.0 mg. While diabetic patients have an increased risk of vascular accidents, including stroke and myocardial infarcts, the potential for adverse effects following IVT administration of pegaptanib is minimized relative to pan-VEGF-A blockers due to its low systemic exposure and selective blocking of $VEGF_{165}$.[25]

Acknowledgments

Author contributions

All authors contributed toward data analysis, drafting, revising, and approving the final version of the paper and agree to be accountable for all aspects of the work.

Disclosure

ASB, DJN, and KYG are full-time employees of Pfizer Inc. Pfizer Global Research and Development funded the individual PK studies that were conducted at multiple investigator centers under the single umbrella of protocol EOP1005. These center-based PK studies were combined into the single analysis described in this report. MMH and KGK, employees of Ann Arbor Pharmacometrics Group, were paid consultants to Pfizer for the development of the PK models. The authors report no other conflicts of interest in this work.

References

1. Aiello LP, Bursell SE, Clermont A, et al. Vascular endothelial growth factor-induced retinal permeability is mediated by protein kinase C in vivo and suppressed by an orally effective beta-isoform-selective inhibitor. *Diabetes*. 1997;46(9):1473–1480.
2. Wild S, Roglic G, Green A, Sicree R, King H. Global prevalence of diabetes estimates for the year 2000 and projections for 2030. *Diabetes Care*. 2004;27(5):1047–1053.
3. Weis SM, Cheresh DA. Pathophysiological consequences of VEGF-induced vascular permeability. *Nature*. 2005;437(7058):497–504.
4. Dvorak HF, Nagy JA, Feng D, Brown LF, Dvorak AM. Vascular permeability factor/vascular endothelial growth factor and the significance of microvascular hyperpermeability in angiogenesis. *Curr Top Microbiol Immunol*. 1999;237:97–132.
5. Ishida S, Usui T, Yamashiro K, et al. VEGF164 is proinflammatory in the diabetic retina. *Invest Ophthalmol Vis Sci*. 2003;44(5):2155–2162.
6. Qaum T, Xu Q, Joussen AM, et al. VEGF-initiated blood-retinal barrier breakdown in early diabetes. *Invest Ophthalmol Vis Sci*. 2001;42(10):2408–2413.
7. Tolentino MJ, McLeod DS, Taomoto M, Otsuji T, Adamis AP, Lutty GA. Pathologic features of vascular endothelial growth factor-induced retinopathy in the nonhuman primate. *Am J Ophthalmol*. 2002; 133(3):373–385.
8. Amin RH, Frank RN, Kennedy A, Eliott D, Puklin JE, Abrams GW. Vascular endothelial growth factor is present in glial cells of the retina and optic nerve of human subjects with nonproliferative diabetic retinopathy. *Invest Ophthalmol Vis Sci*. 1997;38(1):36–47.
9. Funatsu H, Yamashita H, Noma H, Mimura T, Yamashita T, Hori S. Increased levels of vascular endothelial growth factor and interleukin-6 in the aqueous humor of diabetics with macular edema. *Am J Ophthalmol*. 2002;133(1):70–77.
10. Macugen® (pegaptanib sodium injection) [prescribing information]. Palm Beach Gardens, FL: Eyetech Inc; 2011.
11. Reyderman L, Stavchansky S. Pharmacokinetics and biodistribution of a nucleotide-based thrombin inhibitor in rats. *Pharm Res*. 1998;15(6): 904–910.
12. Geary RS. Antisense oligonucleotide pharmacokinetics and metabolism. *Expert Opin Drug Metab Toxicol*. 2009;5:381–391.
13. Tucker CE, Chen LS, Judkins MB, Farmer JA, Gill SC, Drolet DW. Detection and plasma pharmacokinetics of an anti-vascular endothelial growth factor oligonucleotide-aptamer (NX1838) in rhesus monkeys. *J Chromatogr B Biomed Sci Appl*. 1999;732(1):203–212.
14. Healy JM, Lewis SD, Kurz M, et al. Pharmacokinetics and biodistribution of novel aptamer compositions. *Pharm Res*. 2004;21(12):2234–2246.
15. Molitch ME, DeFronzo RA, Franz MJ, et al; American Diabetes Association. Nephropathy in diabetes. *Diabetes Care*. 2004;27:S79–S83.
16. Lindeman RD, Tobin J, Shock NW. Longitudinal studies on the rate of decline in renal function with age. *J Am Geriatr Soc*. 1985;33(4): 278–285.
17. Loftus JV, Sultan MB, Pleil AM; Macugen 1013 Study Group. Changes in vision- and health-related quality of life in patients with diabetic macular edema treated with pegaptanib sodium or sham. *Invest Ophthalmol Vis Sci*. 2011;52(10):7498–7505.
18. Beal SL, Sheiner LB, Boeckmann A, Bauer RJ. *NONMEM User's Guides (1989–2009)*. Ellicott City, MD: Icon Development Solutions; 2009.
19. MathSoft, Inc. *S-Plus for Windows*. Seattle, WA: Data Analysis Division, MathSoft, Inc; 2005.
20. Ahn JE, Karlsson MO, Dunne A, Ludden TM. Likelihood based approaches to handling data below the quantification limit using NONMEM VI. *J Pharmacokinet Pharmacodyn*. 2008;35(4):401–421.
21. Beal SL. Ways to fit a PK model with some data below the quantification limit. *J Pharmacokinet Pharmacodyn*. 2001;28(5):481–504.
22. Stratford RE Jr, Carson LW, Dodda-Kashi S, Lee VH. Systemic absorption of ocularly administered enkephalinamide and inulin in the albino rabbit: extent, pathways, and vehicle effects. *J Pharm Sci*. 1988;77(10):838–842.
23. Kowalski KG, Hutmacher MM. Efficient screening of covariates in population models using Wald's approximation to the likelihood ratio test. *J Pharmacokinet Pharmacodyn*. 2001;28(3):253–275.
24. Basile AS, Hutmacher M, Nickens D, et al. Population pharmacokinetics of pegaptanib in patients with neovascular, age-related macular degeneration. *J Clin Pharmacol*. 2011;52(8):1186–1199.
25. Morjaria R, Chong NV. Pharmacokinetic evaluation of pegaptanib octasodium for the treatment of diabetic edema. *Expert Opin Drug Metab Toxicol*. 2014;10(8):1185–1192.

Supplementary materials

**Table S1** Nominal schedule of plasma sampling for pharmacokinetic analysis

Schedule for the first dose	Schedule for the third dose
Predose	Predose (week 12 prior to dosing)
4±2 hours (day 0)	4±2 hours postdose (week 12)
24±4 hours (day 0)	24±4 hours (week 12)
Week 1±3 days	Week 13±3 days
Week 3±3 days	Week 15±3 days
Week 6 (just prior to second dose)	Week 18 (just prior to fourth dose)

Table S2 Number of patients, observations, BLQs, and exclusions

Sample type		Pegaptanib dose group			Total
		0.3 mg	1.0 mg	3.0 mg	
Patients	n	20	23	15	58
	Row, %	34.5	39.7	25.9	100
Observations					
>BLQ	No. of PK samples	102	173	131	406
	%	18.4	31.2	23.6	73.2
	Row, %	25.1	42.6	32.3	–
	Col, %	52.6	80.8	89.1	–
≤BLQ	No. of PK samples	92	40	12	144
	%	16.6	7.2	2.2	26.0
	Row, %	63.9	27.8	8.3	–
	Col, %	47.4	18.7	8.2	–
Excluded[a]	No. of PK samples	0	1	4	5
	%	0.00	0.18	0.72	0.90
	Row, %	0.00	20.0	80.0	–
	Col, %	0.00	0.47	2.72	–
Total	No. of PK samples	194	214	147	555
	%	35.0	39.6	26.5	100

**Note:** [a]Excluded from the analysis.
Abbreviations: BLQ, below the lower limit of quantification; No., number; PK, pharmacokinetic; Col, column.
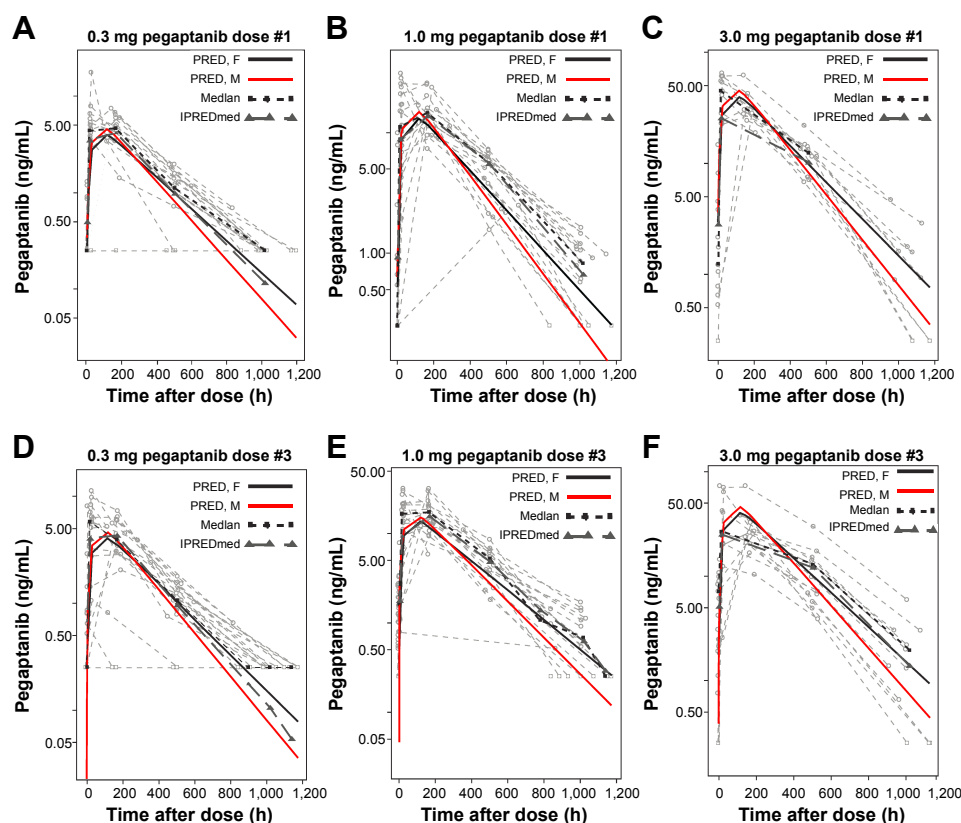
Figure S1 Time course of the observed and predicated plasma pegaptanib concentrations.
Notes: Data presented from samples obtained after the first and third doses, respectively, of pegaptanib (a and d) 0.3 mg, (b and e) 1.0 mg, and (c and f) 3.0 mg, per eye. Gray circles represent concentrations below the lower limit of quantification (BLQ); gray squares represent concentrations equal to or less than BLQ. Model predications plotted here determined using the final model assuming a fixed dosing interval of 6 weeks. The median and IPREDmed were calculated by time-interval bins. For visual clarity, only statistics with more than five observations are plotted.
Abbreviations: F, females; h, hours; IPREDmed, median of individual PRED prediction; M, males; PRED, prediction.
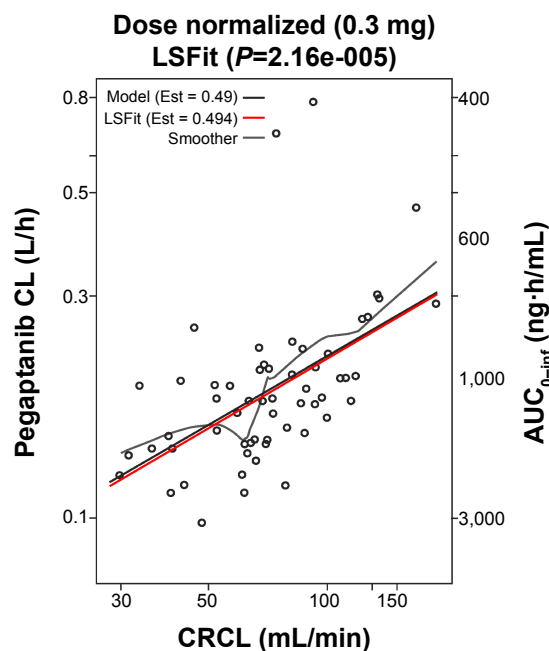
Figure S2 Final model predictions of clearance divided by AUC vs creatinine clearance (CRCL) normalized to the 0.3 mg dose of pegaptanib: (CL/AUC) vs CRCL.
Notes: The plot was composed of dose-normalized data to increase the sample size and improve estimate precision. Model (Est =0.49) is the power parameter from the final model, least squares (LS) regressions were performed for Log^{CL} vs Log^{CRCL}, and the estimate of the slope coefficient is LSFit (Est =0.494). The P-value for the t-test of the LS regression coefficient against the null value of 0 is LSFit ($P<0.0001$). A smoother is also provided. These analyses were performed using S-Plus (TIBCO Software, Palo Alto, CA, USA).
Abbreviations: AUC, area under the concentration–time curve; AUC_{0-inf}, AUC from time 0 to infinity; CL, clearance; Est, estimated slope; h, hour; min, minute; LSFit, least squares regression fit; log^{CL}, log of clearance; log^{CRCL}, log of creatinine clearance; vs, versus.
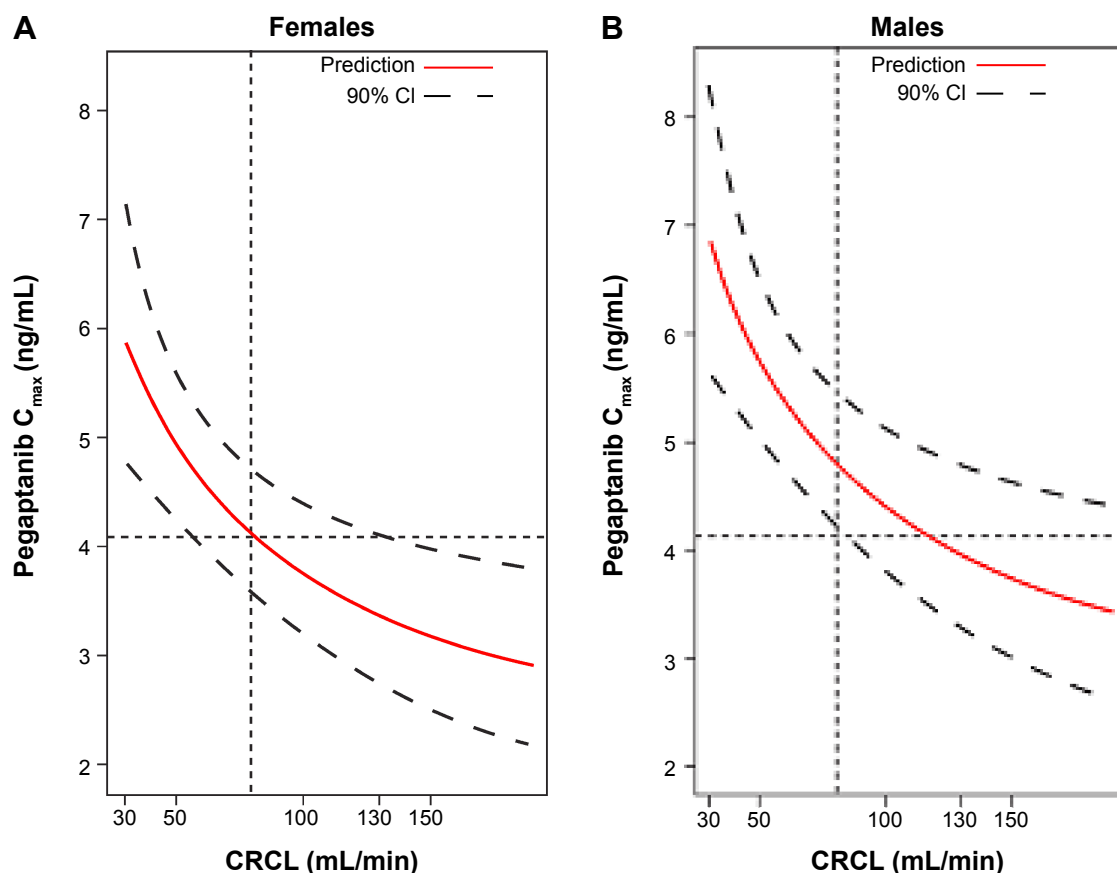
Figure S3 The influence of sex on the relationship between the predicted maximum concentration (C_{max}) of pegaptanib and creatinine clearance (CRCL).
Notes: CRCL was previously found to influence clearance and thus, C_{max}, the influence of CRCL on the predicted C_{max} after a single, 0–3 mg dose of pegaptanib in (**A**) females and (**B**) males. The dashed line represents the 90% CI. The ratios of C_{max} for CRCL 30 and 190 mL/min are predicted to be twofold in both females and males.
Abbreviations: CI, confidence interval; min, minute.